ORIGINAL PAPER

Volcano-tectonic structures and CO_2-degassing patterns in the Laacher See basin, Germany

Andreas Goepel · Martin Lonschinski · Lothar Viereck · Georg Büchel · Nina Kukowski

Abstract The *Laacher See Volcano* is the youngest (12,900 year BP) eruption center of the Quarternary East-Eifel Volcanic Field in Germany and has formed *Laacher See*, the largest volcanic lake in the Eifel area. New bathymetric data of *Laacher See* were acquired by an echo sounder system and merged with topographic light detection and ranging (LiDAR) data of the *Laacher See Volcano* area to form an integrated digital elevation model. This model provides detailed morphological information about the volcano basin and results of sediment transport therein. Morphological analysis of *Laacher See Volcano* indicates a steep inner crater wall (slope up to 30°) which opens to the south. The *Laacher See* basin is divided into a deep northern and a shallower southern part. The broader lower slopes inclined with up to 25° change to the almost flat central part (maximum water depth of 51 m) with a narrow transition zone. Erosion processes of the crater wall result in deposition of volcaniclastics as large deltas in the lake basin. A large subaqueous slide was identified at the northeastern part of the lake. CO_2-degassing vents (wet mofettes) of *Laacher See* were identified by a single-beam echo sounder system through gas bubbles in the water column. These are more frequent in the northern part of the lake, where wet mofettes spread in a nearly circular-shaped pattern, tracing the crater rim of the northern eruption center of the *Laacher See Volcano*. Additionally, preferential paths for gas efflux distributed concentrically inside the crater rim are possibly related to volcano-tectonic faults. In the southern part of *Laacher See*, CO_2 vents occur in a high spatial density only within the center of the arc-shaped structure *Barschbuckel* possibly tracing the conduit of a tuff ring.

Keywords *Laacher See Volcano* · East-Eifel Volcanic Field · CO_2 vents · Bathymetry

Introduction

The Quaternary East-Eifel Volcanic Field (EEVF) is located in the western part of Germany (Fig. 1). In a region of about 400 km^2, at least 103 volcanoes have been mapped (Ahrens 1932; Duda and Schmincke 1978; Frechen 1971; Goepel 2008; Schmincke 1977; van den Bogaard and Schmincke 1990b; Viereck 1984), which erupted in six major phases between >650,000 year BP and about 12,900 year BP (Schmincke 1996; Schmincke et al. 1999; van den Bogaard and Schmincke 1985, 1990a). Two-thirds of the generally K-rich magmas were of melilithic, nephelinitic, leucititic and basanitic-tephritic composition, whereas one-third had intermediate and phonolitic compositions, respectively. The *Laacher See Volcano*, located close to *Maria Laach Abbey* (Fig. 1), explosively erupted about 6.3 km^3 of phonolitic magma during a dominantly phreato-plinian series of eruptions at about 12,900 year BP (Harms and Schmincke 2000; Schmincke et al. 1999; van den Bogaard and Schmincke 1990a). First eruptions of the *Laacher See Volcano* started in the south and later moved toward the northern part of the *Laacher See* basin Schmincke et al. (1999). As a result, the crater of *Laacher See Volcano* was predominantly formed by vent erosion and collapse. Later, the crater was filled with water due to groundwater inflow.

A. Goepel (✉) · M. Lonschinski · L. Viereck · G. Büchel · N. Kukowski
Institute of Geosciences, Friedrich Schiller University, Burgweg 11, 07749 Jena, Germany
e-mail: andreas.goepel@uni-jena.de

Fig. 1 Topographic map of the East-Eifel Volcanic Field in Germany showing eruptive centers after Ahrens (1932), Duda and Schmincke (1978), Frechen (1971), Goepel (2008), Schmincke (1977), van den Bogaard and Schmincke (1990b) and Viereck (1984). The *white rectangle marks* the *Laacher See Volcano* with *Laacher See*, covering an area of 3.315 km². Geographic coordinates are given in *longitude* and *latitude* (WGS84) as well as in UTM 32N
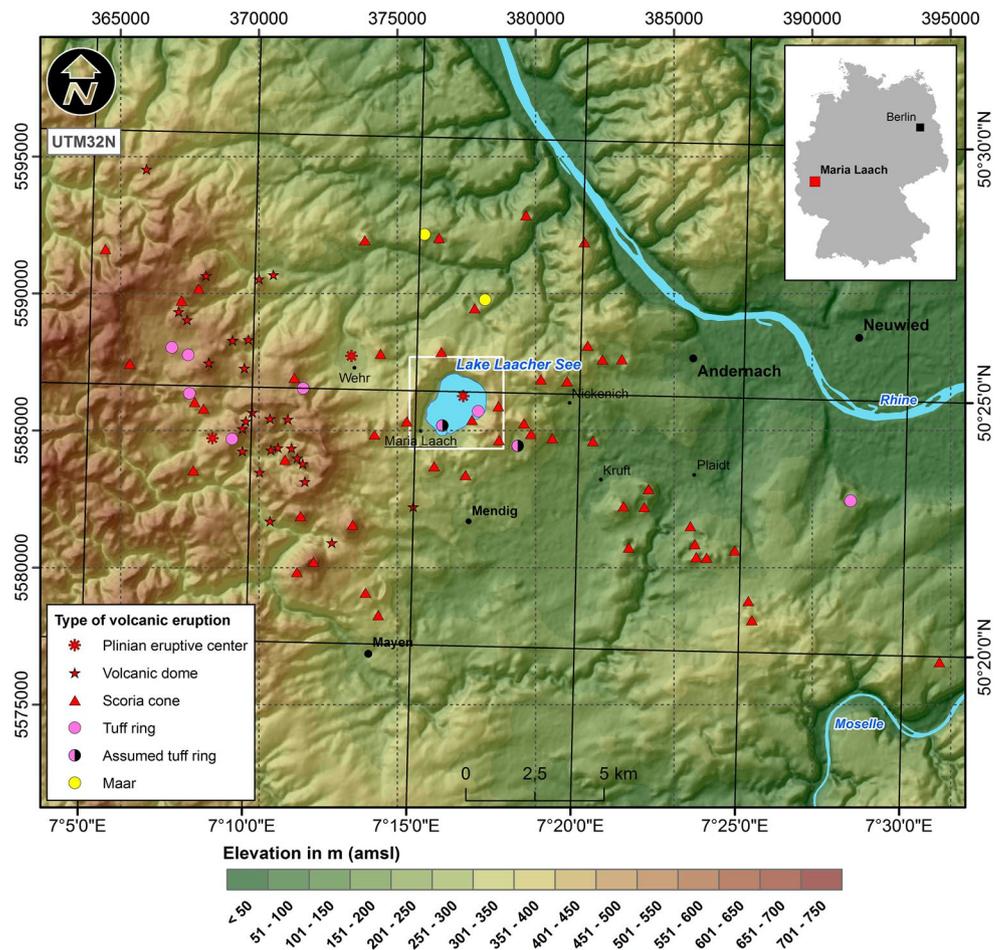
The recent lake level of 275.3 m (amsl) is maintained by a drainage system, controlled by an overflow through the manmade gallery *Deliusstollen* which was finished in 1845 AD (Grewe 1979). However, anthropogenic water management through the last centuries influenced *Laacher See*. Historical records show that first attempts to lowering the lake level from 288 to 278 m (amsl) were realized in 1167 AD by finishing the drainage gallery *Fulbertstollen* (Grewe 1979).

The *Laacher See* is holomictic (Scharf 1987), i.e., a complete vertical mixing of the water body occurs at least once a year, but an annual stratification is formed during the summer months. During our study in August and September 2010, a lake stratification into epilimnion, metalimnion and hypolimnion had been established (Fig. 2).

The Quaternary East- and West-Eifel volcanic fields are accompanied by numerous highly mineralized springs (Na–Mg–Ca–K–HCO$_3^-$-type acidulous water) with a CO_2 concentration of more than 250 mg kg^{-1} (H$_2$O) (Carlé 1975; May 2002). Discharge of CO_2 gas (wet mofettes) in the *Laacher See* has been known for many years (e.g., Frechen et al. 1967; Giggenbach et al. 1991; Meyer 1994; Pfanz 2008). Giggenbach et al. (1991) analyzed the gas phase and found besides CO_2 (990 mmol mol^{-1}) also N$_2$
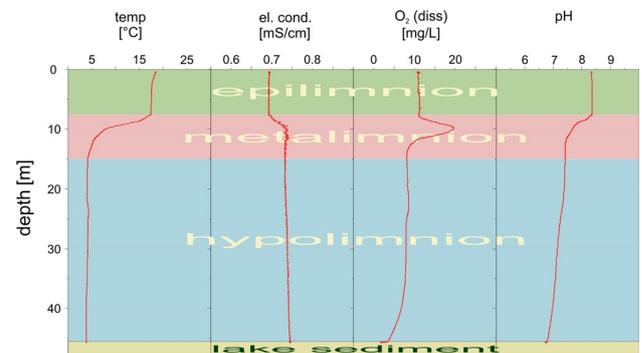
Fig. 2 Water column profiles of temperature, electrical conductivity, dissolved oxygen and pH value in *Laacher See* on August 1, 2010, at 12:00 p.m. MEZ

(5 mmol mol^{-1}), CH$_4$ (1 mmol mol^{-1}) and noble gases. Nevertheless, CO_2 plumes in the lake have been mentioned mainly at the northeastern part of the lake close to the shoreline. At this particular area on the eastern side of the lake, numerous vents (dry mofettes) with CO_2 contents higher than 90 % in the soil gas are widespread (Pfanz 2008; Stoiber-Lipp et al. 2012). Dry mofettes are also known

from a small area along the western lake side (Gal et al. 2011). Hernández et al. (2010) estimated a CO_2 efflux from *Laacher See* to be about 14.04 t km^{-2} d^{-1}. This amount is relatively low in comparison with the CO_2 emission of other volcanic lakes with neutral pH conditions worldwide (mean: 201.1 t km^{-2} d^{-1}, Pérez et al. 2011). Studies of $^3He/^4He$ ratios and $\delta^{13}C$ values of CO_2 in the *Laacher See* indicate a mantle signature (Aeschbach-Hertig et al. 1996; Giggenbach et al. 1991). The efflux of CO_2 from the mantle could be linked to feeder dikes that serve as short cuts in the layered crust or to tectonic structures. Similar CO_2-degassing pattern in the West-Eifel Volcanic Field (WEVF) has been found to be related to tectonic structures (May 2002). Correlations between CO_2 efflux and the trending direction of local volcanic structures are described, for example, for the *Cuicocha* volcano in Ecuador (Padrón et al. 2008) and for the *Miyakejima* volcano in Japan (Hernández et al. 2001).

CO_2 bubbles in lake water can be identified with an echo sounder system. This method has been successfully applied in the previous studies, e.g., Cardigos et al. (2005) utilized an 28 kHz echo sounder to indicate vent bubble plumes close to the *Azores*, Canet et al. (2010) found flares of gas bubbles in the *Gulf of California* by an 18 kHz sounder, and Bernard (2011) used an 50 kHz echo sounder for the investigation of CO_2 degassing at the *Taal* volcano, Philippines. Wessels et al. (2010) used various hydroacoustic tools, including sidescan sonar and multibeam echo sounder, to study pockmarks caused by methane degassing at the lake ground of Lake Constance. In bubble release experiments performed at *Lake Lucerne* in combination with discrete bubble modeling, McGinnis et al. (2011) confirmed that bubbles of CO_2 dissolve rapidly and released CO_2 tend to remain near the lake floor.

Bathymetric surveys in volcanic lakes are a suitable tool to identify volcanic features to unravel the recent and historic volcanic activity. For example, hydrothermal explosion craters, hydrothermal vents, sublacustrine landslide deposits and submerged former shorelines in the *Yellowstone Lake* were identified based on a multibeam sonar mapping (Morgan et al. 2003). The lake morphology of the *Kawah Ijen* volcano crater lake in Indonesia was compared to historical morphological records to estimate changes in the underwater volcanic activity to improve the prediction of future eruptions (Takano et al. 2004). Anzidei et al. (2008) recognized five underwater crater structures and former submerged shorelines for the *Colli Albani* volcano in Italy revealed by echo sounder surveys. Recently, joint digital elevation models (DEM), bathymetric data and seismic surveys are increasingly being used to perform morphometric data analysis (e.g., slope analysis) to discover concealed volcanic structures (e.g., Fornaciai et al. 2012; Grosse et al. 2012; Ross et al. 2014). In addition, morphometric analysis is used to identify topographic attributes and sedimentological structures as well. For example, Ulusoy et al.

(2004) studied the volcano-structural properties of the *Bodrum* peninsula (Turkey) by morphometric analysis of DEM images. DEM data are also very useful in the investigation of landslides (e.g., Guzzetti et al. 2012).

The aim of our study was to map the spatial distribution of CO_2-degassing vents within *Laacher See* and provide additional information on volcanic and sedimentological features by joint analysis of bathymetric and DEM data.

Methods

Conductivity–temperature–depth probe (CTD) measurements and hydrochemistry

To determine the temperature-related lake stratification, conductivity, temperature and depth measurements in the water column were conducted on August 1, 2010, at 12.00 p.m. MEZ. The measurements were performed using a CTD90M (Sea and Sun Technology), equipped with sensors for pH and O_2 acquisition, additionally. The CTD was used in a continuous mode with a sampling rate of 5 Hz. The probe was moved down with a hand-operated winch with a speed of about 0.05 m s^{-1}. Acquisition of these parameters is essential to correct sonic wave velocity, which, e.g., depends on temperature.

Water samples were collected on August 14, 2010, in five different depths: 1, 2, 12.5, 20 and 40 m in order to determine the hydrochemistry of *Laacher See*. Therefore, a FreeFlow water sampler (Hydro-Bios) with a sample volume of 5 L and a hand-operated winch with a mechanical counter was used to determine the water depth.

Dissolved CO_2 was determined directly after sampling by titration (with NaOH solution) using a Digital Titrator Kit (Hach) and a portable device WTW pH320 (Xylem) for pH measurements with pH probe (Pt-electrode and KCl solution, Schott).

Samples for anions (except for HCO_3^-) and elements were filtered using glass fiber prefilters (Sartorius) and cellulose acetate filters (0.45 µm, Sartorius). Water samples for element analysis finally were acidified with HNO_3 (65 %, subboiled) to pH < 2. All samples were kept at 6 °C until they were analyzed.

HCO_3^- was analyzed at the day of sampling by titration of total alkalinity (Titrino 716 DM, Metrohm USA Inc.), whereas Cl^-, F^-, NO_3^- and SO_4^{2-} were analyzed by ion chromatography (DX-120, Dionex). PO_4^{3-} was determined by spectrophotometer DR/4000 U (Hach). The elements Ca, K, Mg, Na, Si and Sr were determined by inductively coupled plasma optical emission spectrometry (ICP-OES; Varian 725 ES). Inductively coupled plasma mass spectrometry (ICP-MS; X-Series II, ThermoFisher Scientific) was used to analyze Fe and Mn.
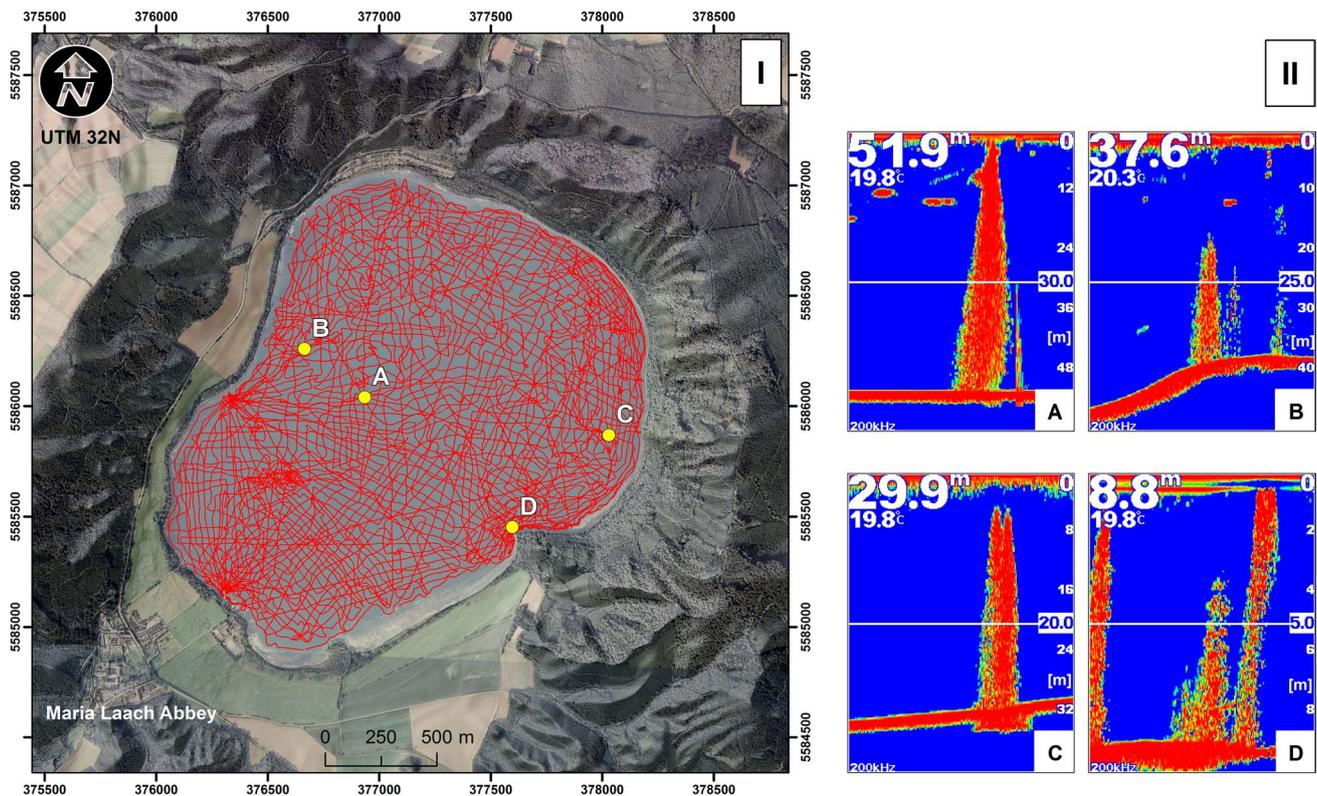
Fig. 3 I Tracks of the echo sounder mapping (total length: 235 km) are indicated by the *red lines*. The digital elevation model of *Laacher See Volcano* is superimposed by an aerial photo (data provided by "Landesamt für Vermessung und Geobasisinformation Rheinland-Pfalz (LVermGeo)"). **II** Screenshots of the echo sounder signatures of gas bubble plumes (*A–D*). The scales on the images (*right side*) indicate water depth (m) and surface water temperature (°C)

Bathymetry and topography

Laacher See floor bathymetric data were acquired using an echo sounder GARMIN GPSMap 421s utilizing a 500 W dual-frequency transducer single-beam. The transducer has a beam width of 10° at 200 kHz or 40° at 50 kHz, respectively, and was mounted at the bottom of a float (0.05 m below lake level). This device has a dimension of 1 m by 0.5 m and consists of a polypropylene foam core encapsulated by a plastic bottom. This setup minimizes wave-induced roll and pitch movements of the transducer very effectively. Above the transducer, a GARMIN GA25 GPS antenna was mounted to acquire the geographic position. Data were collected on profiles with an average speed of 4 km h^{-1} (total length of 235 km, Fig. 3) and stored at a sampling rate of 1 Hz on a custom-made external data logger. The transducer was operated at 200 kHz in single-beam mode only, which results in a sweep cone with a maximum diameter of approximately 18 m at a depth of 50 m. Since the sounder is calibrated to be used in salt water (wave velocity: 1,500 m s^{-1}; GARMIN 2012), a correction of the raw depth data was necessary. To do so, we applied a numerical model using the equation for the speed of sound in salt water (Wilson 1960) incorporating the temperature–depth curve of *Laacher See* from August 2010 (Fig. 2), the hydrostatic pressure (depending on water depth) and a constant salinity of 0.4 ‰. The sounder system has a vertical measuring accuracy of 0.3 m (GARMIN 2012). During data acquisition, *Laacher See* lake level was constant at 275.3 m (amsl) as measured by a Topcon GR5 Differential Global Positioning System (DGPS). Bathymetric data (available in Supplement A) were interpolated to a raster on a 10-m regular grid using kriging algorithm (12 neighbors, search radius 100 m) of software package ArcGIS v. 9.3.1 (ESRI). Bathymetric volume calculations were also performed using ArcGIS v. 9.3.1 (ESRI).

Terrestrial topographic data used in this study are derived by airborne acquired high-resolution point cloud data (LiDAR). These data have a resolution of at least four dots per square meter with a position accuracy of 0.3 m and contain vegetation as well as ground points (Landesamt für Vermessung und Geobasisinformation Rheinland-Pfalz, LVermGeo). No ground filtering algorithms were applied to remove vegetation points. LiDAR data were gridded to a raster with a cell size of 1 m using software package ArcGIS v. 9.3.1 (ESRI) featuring the 3D Analyst Terrain

toolset (ESRI). Slope analysis was performed using the 3D Analyst toolsets (ESRI).

Bathymetric (echo sounder) and topographic (LiDAR) data support different spatial resolutions. Our bathymetric data have a maximum spatial resolution of 10 m, whereas LiDAR data provide a resolution which is 10 times higher. To permit a joint interpretation of both data sets, a new seamless 1 m spaced DEM was gridded whereby bathymetric data were extrapolated to an equal grid size.

CO_2-degassing vents (wet mofettes)

The echo sounder signals (specification identical to bathymetric measurements) reflect rising gas bubbles. Figure 3 displays examples of typical degassing spots at the lake bottom forming nearly vertical flares. In this way, the method is suitable to localize CO_2 vents in the *Laacher See*. All vents reported here (e.g., Fig. 7) were detected on the monitor of the sounder, and the geographic position was recorded. The measurements were taken in August and September 2010. The spatial distribution of the CO_2 vents was stable during the entire time period of our study as observed from repeated survey along the same profiles.

Results

Conductivity–temperature–depth probe (CTD) measurements and hydrochemistry

During the entire time period of our study, *Laacher See* showed three-layer temperature stratification; the epilimnion was built down to 7.5 m water depth, the metalimnion was found from 7.5 to 15 m water depth, and the water body below 15 m depth characterized the hypolimnion (Fig. 2). Values of electrical conductivity increased from 0.69 mS cm^{-1} in the epilimnion to 0.74 mS cm^{-1} in the metalimnion and remained almost constant at this value in the hypolimnion. Concentration of dissolved oxygen was saturated at 10 mg L^{-1} in the epilimnion and reached maximum values of 20 mg L^{-1} at 10 m water depth in the metalimnion. The hypolimnion shows oxygen contents of 8 mg L^{-1} down to 35 m water depth and decreasing oxygen concentrations to values lower 2 mg L^{-1} close to the lake bottom. The pH value was constant at 8.3 in the epilimnion and dropped to 7.5 in the metalimnion. The hypolimnion shows pH values decreasing with water depth, whereby lowest pH values (6.8) were found close to the lake bottom.

Concentrations of dissolved CO_2 increased with water depth. Highest concentrations (54.5 mg L^{-1}) were detected at 40 m water depth, 16.4 mg L^{-1} at 20 m water depth and 11.6 mg L^{-1} at 12.5 m water depth. No dissolved CO_2 was found at 1 and 2 m water depth (Table 1). Further element

Table 1 Concentrations of dissolved CO_2, elements and anions in different water depths of *Laacher See*

Sampling depth (mg L^{-1})	1 m	2 m	12.5 m	20 m	40 m
CO_2	0	0	11.6	16.4	54.5
Ca	40	40.1	44.1	43.9	44.1
Fe	0.0015	0.0018	<0.0008	<0.0008	0.001
K	25.2	25.5	25.1	25.2	24.6
Mg	34.9	35	34.7	34.5	34.4
Mn	0.0015	0.0015	0.0008	0.0008	0.0016
Na	46.5	46.8	46.5	46.3	45.4
Si	0.45	0.42	1.06	1.07	1.67
Sr	0.52	0.52	0.53	0.53	0.52
F$^-$	0.48	0.48	0.48	0.48	0.49
Cl$^-$	18.62	18.47	18.22	18.13	18.19
SO$_4^{2-}$	26.8	26.6	26.5	26.5	25.7
NO$_3^-$	0.9	0.4	0.4	0.4	0.4
PO$_4^{3-}$	<0.05	<0.05	<0.05	<0.05	0.25
HCO$_3^-$	384.1	378.9	406.6	406.2	408.4

and anion concentrations are depicted in Table 1, but will not be discussed in detail since this study is not focused on this topic. Generally, most species have the same concentration along the entire water column with the exception of Ca and HCO$_3^-$, which are lower at 1 and 2 m water depth.

Bathymetry and topography

The crater of *Laacher See Volcano* is expressed as a lake basin with a maximum water depth of 51 m (Fig. 4). The recent water body of *Laacher See*, 0.103 km^3 in volume, covering an area of 3.309 km^2 with an 8.471 km long shoreline (Table 2). *Laacher See* basin is surrounded by an elongated crater wall with a northeast–southwest extension of 3,800 m and a northwest–southeast extension of approximately 3,000 m (Fig. 5). The crater wall rim extends 160 m above the lake level of 275.3 m (amsl), at a distance of 300–700 m from the shoreline. In the southwest, the crater wall rim is strongly eroded. The inner crater walls are very steep (with slopes up to 30°) and characterized by a number of gullies as a result of intense erosion (Fig. 6). The outer crater wall has an average slope of about 15° and thus shows a much flatter morphology. Due to erosion, the crater wall is open to the southwest through the valley of the creek *Beller Bach* (loc. A in Fig. 5), but also to the northwest (loc. C in Fig. 5), and southeast (loc. L and K in Fig. 5). The lake basin is shaped like an hourglass and divided into a shallower (down to 44 m water depth) southwest part and a deeper (down to 51 m water depth) northeast part (Figs. 4, 5). Generally, the lake bottom drops toward the central lake basin with a slope up to 25° (Fig. 6).

Fig. 4 Simplified bathymetric map of *Laacher See*. *Numbers* besides the isobaths indicate the water depth (m) below lake level (275.3 m amsl)
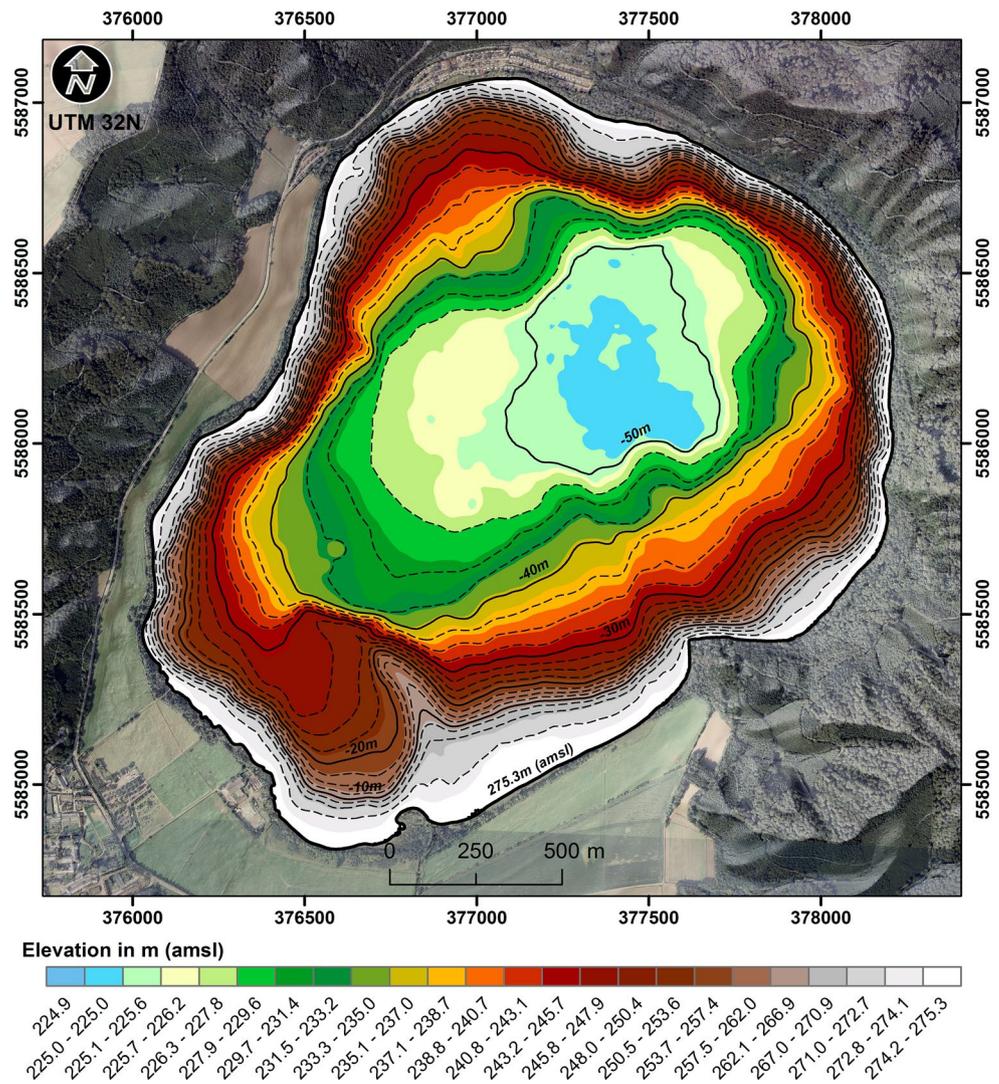
Elevation in m (amsl)

Table 2 Area and volume calculation for various shorelines based on the digital elevation model

Shoreline age in years AD	Elevation in m (amsl)	Area in km²	Volume in km³	Change based on present lake level	
				Δ Area (%)	Δ Volume (%)
1845[a] to present (see SL1 in Fig. 6)	275.3	3.3085	0.1029	no change	no change
1167[b] (see SL2 in Fig. 6)	278.0	3.7593	0.1126	+13.6	+9.4
Thirteenth century[c] (see SL3 in Fig. 6)	283.0	4.2399	0.1326	+28.2	+28.9
Before 1167 (see SL4 in Fig. 6)	288.0	4.6331	0.1548	+40.0	+50.4

[a] 1845 AD—finished construction of gallery *Deliusstollen* (Grewe 1979)

[b] 1167 AD—finished construction of gallery *Fulbertstollen* (Grewe 1979)

[c] Accidental collapse of gallery *Fulbertstollen* (Grewe 1979)

In the central northern part of the lake, a flat area at about 50 m water depth (Fig. 4, location I in Fig. 5) has been identified. It is stretched over 1,000 m in northeast–southwest direction and 500 m in northwest–southeast direction. Furthermore, an arc-shaped ridge of about 600 m length and 50–70 m width (location F in Fig. 5) in the southern lake basin marks the so called *Barschbuckel*. The ridge extends approximately 20–25 m above the lake ground. In the north of the *Barschbuckel*, three humps (up to 4 m high) with diameters up to 60 m were identified (loc. D in Fig. 5).
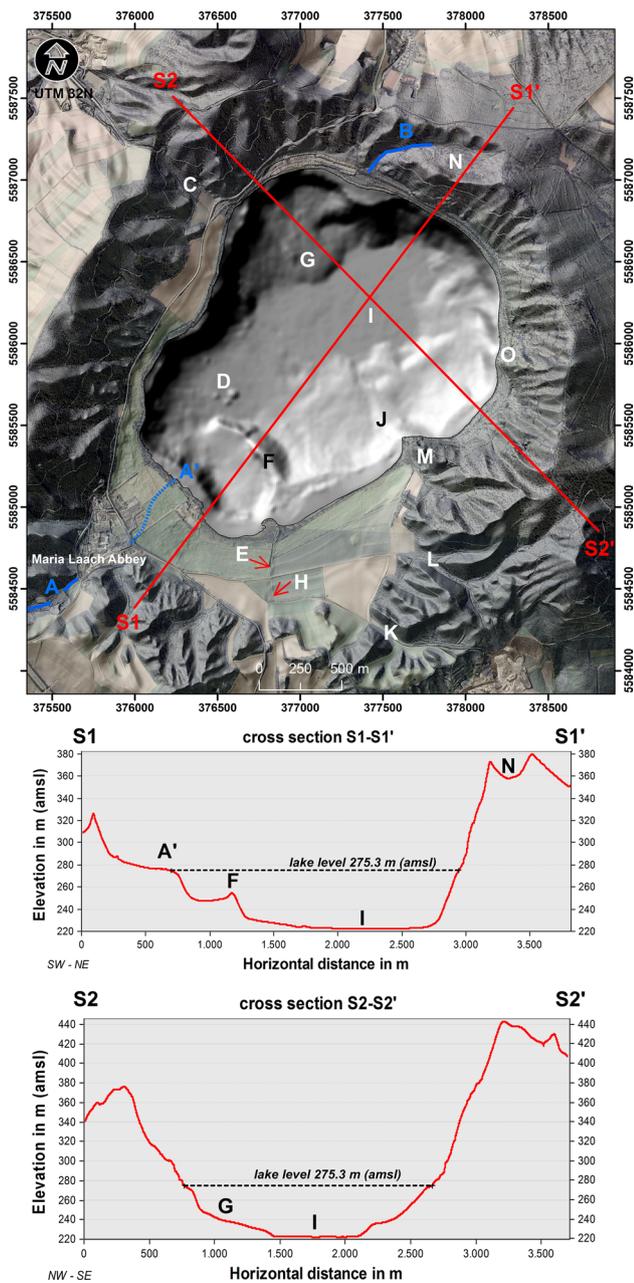
Fig. 5 Hillshade image (azimuth: 315°, elevation: 45°, vertical exaggeration (VE) = 5) of digital elevation model including the bathymetric model of the *Laacher See* basin. Cross sections S1–S1′ and S2–S2′ with VE = 3. *Denotations*: A, valley of creek *Beller Bach*; A′, mouth of creek *Beller Bach*; B, intermitting creek *Im Unselt*; C, *Mohlenberg* valley; D, humps; E, entrance gallery *Deliusstollen*; F, *Barschbuckel*; G, subaqueous slide, *white line contours* the slide body (volume approximately: 3.65 10⁶ m³); H, collapsed entrance gallery *Fulbertstollen*; I, deep lake plain; J, *Jägerspitze*; K, L, unnamed erosion valleys; M, scoria cone *Alte Burg*; N, erosion valley *Im Unselt*; O, lava flow *Lorenzfelsen*

A number of deltas were deposited in the littoral zones around the shoreline of *Laacher See* (locations: D1–D6 in Fig. 6). The horizontal extents of the deltas range from 300

to 600 m, and the progradations into the lake reach from 100 to 150 m. A major subaqueous slide with a rough surface topography was identified in the northwestern part of the lake (loc. G in Fig. 5). It is spread over 700 m in width and up to 600 m into the lake.

From local slope gradients (Fig. 6), former shorelines of the lake can be identified. SL1 (Fig. 6) marks the recent lake level at 275.3 m (amsl). SL2 (Fig. 6) is at 278.0 m (amsl) and runs above the entrance to the manmade gallery *Deliusstollen* (entrance: loc. E in Fig. 5). A further line is at 283.0 m (loc. SL3 in Fig. 6), and the oldest paleo-shoreline (loc. SL4 in Fig. 6) is located at an elevation of about 288.0 m (amsl).

CO₂-degassing vents (wet mofettes)

In addition to the acquisition of bathymetric data, rising gas bubbles (wet mofettes) were identified along profiles throughout the *Laacher See* basin (Fig. 7). The number of wet mofettes is considerably higher in the northeastern part of the lake basin with a patchy distribution of CO₂-degassing vents. Nevertheless, localized zones with a high density of vents were identified on the eastern shore close to the *Jägerspitze* (loc. J in Fig. 5), between the scoria cone *Alte Burg* (loc. M in Fig. 5) and the lava flow of *Lorenzfelsen* (loc. O in Fig. 5) as well north of *Lorenzfelsen* close to the lakeshore. In the immediate vicinity of the eastern shoreline (north of *Lorenzfelsen*) at a length of 1,000 m, degassing vents are directly visible as fields of gas bubbles. In the northwestern part of the lake, we found several areas with a higher density of wet mofettes at a distance from 150 m up to 500 m from the western shore (Fig. 7). There is a noticeable lack of degassing vents in the central deep part of the basin. Overall, wet mofettes in the northeastern part of the lake basin are spread in an almost circular-shaped pattern with a diameter of about 1.5 km (Fig. 7). We have not identified any wet mofettes in the southwestern lake basin with the exception of a major cluster of degassing vents with a diameter of about 100 m, approximately 130 m offshore from the southwestern shoreline.

Discussion

Physical and chemical properties

Physicochemical measurements in the water column of *Laacher See* indicate a three-layer stratification with constant values in the epilimnion, strong gradients within the metalimnion and a hypolimnion showing constant values for temperature and electrical conductivity, but values for dissolved oxygen and pH decreasing with water depth (Fig. 2). The pH value is strongly related to dissolved CO₂,

Fig. 6 Local slope gradients of the *Laacher See Volcano* basin. D1, delta of creek *Beller Bach*; D2, unnamed delta; D3, delta of *Mohlenberg* valley; D4, delta of creek *Im Unselt*; D5, D6, unnamed deltas; SL1, present lake level 275.3 m (amsl); SL2, lake level formed after first lowering in 1167 AD; SL3, lake level at thirteenth century; SL4, lake level prior 1167 AD
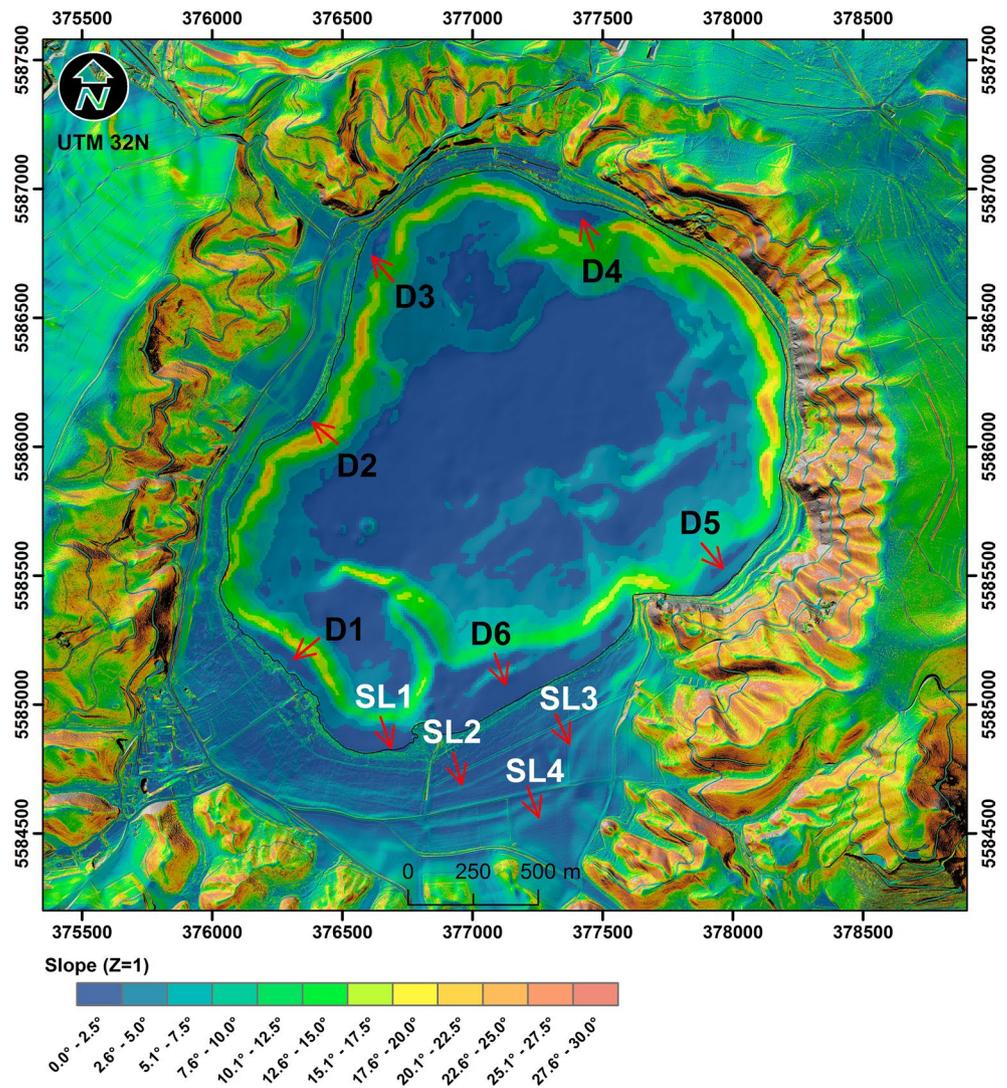
the highest concentrations of which were found close to the lake bottom (Table 1). CO_2 concentrations decrease with decreasing water depth, which is mirrored in pH values. This most probably may be due to parts of the rising CO_2 gas bubbles getting into solution and remaining near the lake bottom. This is consistent with the model of McGinnis et al. (2011), who stated that rising bubbles of CO_2 in lake water should dissolve rapidly and subsequently sink to the lake bottom. Most likely, not all CO_2 bubbles in *Laacher See* get in solution during gas rise, but reach the lake surface. Nevertheless, concentration of dissolved CO_2 in the epilimnion is zero due to CO_2 consuming photosynthesis of algae and other organisms living in the epilimnion. Electrical conductivity of *Laacher See* water was approximately 0.7 mS cm^{-1} and therefore higher than in maar lakes (*Ulmener Maar*: 0.2–0.3 mS cm^{-1}; *Pulver Maar*: 0.1 mS cm^{-1} (Scharf and Oehms 1992) in the WEVF. A chemocline that means a vertical hydrochemical gradient within the water column becomes not evident in *Laacher See* at the time of

measurement. Water chemistry is dominated by Mg, Ca, Na, K and HCO_3^- (Table 1), most likely due to interaction of inflowing groundwater with tephra material, which is abundantly outcropping at the floor of *Laacher See*.

Bathymetry and topography

The bathymetric measurements reveal that the hourglass-shaped basin of *Laacher See* is divided into a shallower and smaller southwestern part and a deeper and larger north-eastern part. This is consistent with the eruptive history of *Laacher See Volcano*, during which the eruptive center moved from the southern part of the basin toward its north-eastern part during volcanic activity (Schmincke 1999). This implies that the products of the later explosive phase buried the initial southern eruption center. The collapse of the volcanic complex at the end of the eruptions led to the very steep crater slopes. Due to post-eruptive sedimentation, the central part of the lake is almost flat. This deep

Fig. 7 Spatial distribution of CO_2 vents (mofettes) in the area of *Laacher See Volcano*. Wet mofettes (*yellow dots*) were identified by an echo sounder; dry mofettes (*red dots*) are soil sampling points with CO_2 contents >90 vol%; *blue crosses* are soil sampling points with CO_2 contents <90 vol%, respectively. Data of dry mofettes are published by Stoiber-Lipp et al. (2012)
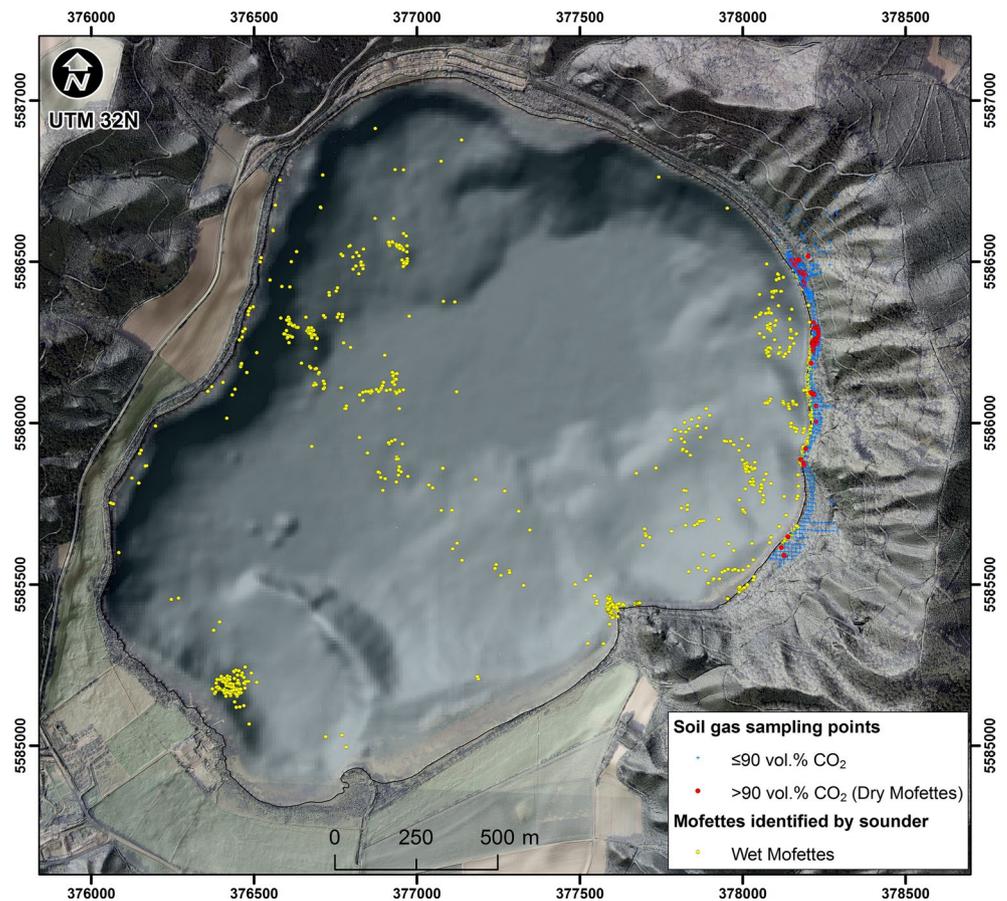
flat has existed most likely already in an early stage of lake formation, similar to maar lakes in the WEVF (Scharf and Menn 1992). The bathymetric model also reveals different morphological features like deltas, subaqueous slides, the *Barschbuckel* ridge and a group of humps of unknown composition and origin on the lake floor.

Erosion of the crater wall of *Laacher See Volcano* has led to the deposition of sediments in the lake basin. As a result, deltas occur offshore the littoral zones of the lake. This is confirmed by sediment cores (Bahrig 1985). To determine the provenance of the sediments the DEM of the *Laacher See* area can be used. In two cases, the observed deltas are related to recently existing creeks. The creek *Beller Bach* (Fig. 5) formed the delta located in the southwest (location D1 in Fig. 6), and the intermittent creek *Im Unselt* is connected to location D4 (Fig. 6) in the northern part of the lake. The flow direction of *Beller Bach* was altered in the last centuries; it now runs into the lake underground between locations A (Fig. 5) and the present-day mouth (loc. A' in Fig. 5). The remaining deltas (D2, D3, D5 and D6 in Fig. 6) originated from sediment input from dry valleys, e.g., *Mohlenberg* valley (loc. C in Fig. 5) or a nameless valley between the lava flow *Lorenzfelsen* (loc. O in Fig. 5) and the scoria cone *Alte Burg* (loc. M in Fig. 5).

The underwater slide (loc. G in Fig. 5) at the northwestern part of the lake was likely caused by instabilities of a former delta. It is also possible that this slide originated from subaerial source areas, such as debris flows into the lake. Turbidities in lake sediment cores, described by Bahrig (1985), may indicate that subaqueous slides occurred within the lake. However, these records are not clear indications since turbidities could also be formed, e.g., by extreme flood events.

The arc-shaped *Barschbuckel* structure (location F in Fig. 5), conspicuously visible in the bathymetric model, has been previously known and interpreted as a ridge of Devonian shale, which already existed before the eruption of the *Laacher See Volcano* (Bahrig 1985). The statements of Bahrig (1985) are based on interpretations of seismic profiles which do not reveal any obvious evidence for an isolated volcanic center at this location. Total magnetic field data (Lorenzen and Berckhemer 1976; Pucher 1992) do not indicate an anomaly related to a separated volcanic center at this location, although the topography of the structure is similar to a partly conserved (possibly palagonized) tuff ring. Therefore, we suggest that the conservation of a preexisting arcuate Devonian ridge at this position seems unlikely. The origin and lithological composition of the

Fig. 8 Sketch of assumed volcano-tectonic elements inside the *Laacher See Volcano* basin. The northern (N) and southern (S) crater rims of *Laacher See Volcano* were first mentioned by van den Bogaard and Schmincke (1990a, b). Based on our newly acquired data of spatial distribution of CO_2-degassing vents the run of the northern (N) crater rim of *Laacher See Volcano* was modified. Preferential paths for gas rise indicate possible volcano-tectonic fault scarps inside the crater rim. The position of the southeastern crater rim of the scoria cone *Alte Burg* and the tuff ring *Graue Ley* (as tuff ring M1) is mentioned in Freundt and Schminke (1984). Based on morphological features and the spatial distribution of wet mofettes, *Barschbuckel* is considered as a partially preserved crater wall of a palagonized tuff ring
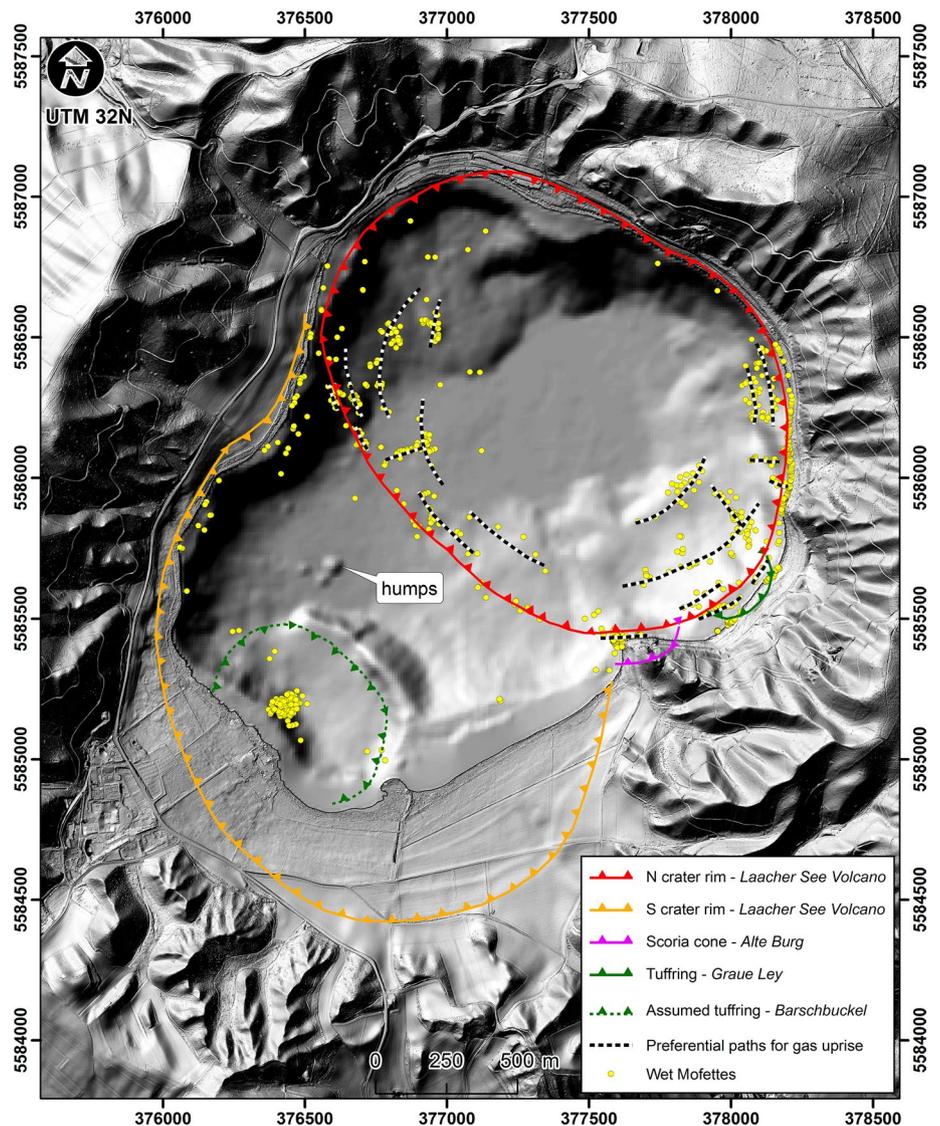
three humps (loc. D in Fig. 5) north of *Barschbuckel* is not unveiled through the data given here, and further investigations are under way.

Between the scoria cone *Alte Burg* (loc. M in Fig. 5) and the lava flow *Lorenzfelsen* (loc. O in Fig. 5), Freundt and Schminke (1984) suggested a phreatomagmatic eruptive center (*Graue Ley* in Fig. 8) based on tuff ring deposits exposed at this area. Based on our bathymetric dataset, the tuff ring *Graue Ley* has to be considered as older than the *Laacher See Volcano*, due to the lack of morphological tuff ring features within the basin of *Laacher See Volcano*.

CO_2-degassing vents (wet mofettes)

The spatial distribution of wet mofettes, in an approximately ring-shaped pattern (Figs. 7, 8), traces the northern crater rim ("N crater rim" in Fig. 7) of the *Laacher See*

Volcano, which could be identified in detail in this study for the first time. The crater rim is likely characterized by volcano-tectonic faults, being preferential flow paths for the uprising CO_2. Based on seismic data, volcano-tectonic faults were also suggested by Bahrig (1985) for the eastern part of *Laacher See*. Magnetic measurements (Lorenzen and Berckhemer 1976) indicate a northwest–southeast elongated positive magnetic anomaly in the northern part of *Laacher See* which most likely is caused by a magmatic body. The absence of CO_2 vents in the central northern part of the lake thus may be a consequence of this magmatic intrusion, which may prevent upward gas flux. The eastern part of the northern crater rim is located close to the eastern shoreline, which is evident by the large number of wet mofettes. In this area, the CO_2 gas flux is increased also onshore, where dry mofettes with CO_2 concentrations higher than 90 vol % in soil gas were found (Pfanz 2008;

Stoiber-Lipp et al. 2012). The spatial distribution of dry mofettes (Fig. 7) is bound up to 30 m sub-parallel to the shoreline (Stoiber-Lipp et al. 2012) and marks the eastern crater rim. Between the lava flow *Lorenzfelsen* and the scoria cone *Alte Burg,* wet mofettes are widespread (Figs. 7, 8). Preferential paths for the gas rise are most likely linked to a conjugated set of faults originating from post-eruptive volcano-tectonic activity. Closer to the shoreline, wet mofettes may be additionally associated with the older tuff ring *Graue Ley* (Fig. 8), which is documented by deposits onshore (Freundt and Schmincke 1984). Widespread clusters of wet mofettes were also found in the western part of the northern crater rim (Fig. 8). We suggest that the distribution of the mofettes is controlled by conjugated faults. Wet mofettes were not identified at the northern lakeside, suggesting that the northern crater rim is located onshore (Fig. 8). Here, further measurements of CO_2 in the soil gas are under way to identify the northern crater rim.

A southern crater rim ("S crater rim" in Fig. 8), representing the first stage of *Laacher See volcano* eruption, was already defined by van den Bogaard and Schmincke (1990a, b). A number of wet mofettes close to the western shoreline are likely associated with the western part of the southern crater rim (Fig. 8). Since the extent of this crater rim in the south and south-east is presently located onshore, wet mofettes cannot be related to the crater rim. Measurements to identify dry mofettes have not been successful up to now. It is conspicuous that in the southern part of the lake, CO_2 vents in high spatial density only occur in an area close to the delta of the creek *Beller Bach* (loc. D1 in Fig. 6). This very small area of degassing approximately marks the geometric center of the circular structure indicated by the *Barschbuckel*. The cause of this degassing pattern thus may mirror the conduit of a possible but not yet confirmed *Barschbuckel* volcanic center.

Historical water management

The run of the former shorelines of the lake on the landside (Fig. 6) is closely related to historical events of water management at the lake (Table 2). Shoreline SL4 (Fig. 6) is located at 288 m (amsl) and represents the lake level prior to 1167 AD, when the lake level was lowered for the first time after completion of the drainage gallery *Fulbertstollen* (Grewe 1979). Since the lake was lowered by about 10 m (Grewe 1979), the new shoreline after 1167 AD was at 278 m (amsl), marked as line SL2 (Fig. 6). Between these shorelines, a further line (loc. SL3 in Fig. 6) was identified at 283 m (amsl). According to historical records, the *Fulbertstollen* had collapsed in the thirteenth century (Grewe 1979), and the lake level temporarily rose to 283 m (amsl). To lower the lake level again, the drainage gallery *Deliusstollen* was finished in 1845 AD (Grewe 1979), resulting in

a new lake level at 273 m (amsl). This level has remained unchanged since then (loc. SL1 in Fig. 6).

Conclusions

Laacher See Volcano is composed of two main craters, overall elongated in northeast–southwest direction and with its lowermost crater rims in the southern part. The general slope of the inner crater wall is twice as steep as the outer crater wall with average values of 15°. Inside the crater of *Laacher See Volcano*, the lake basin has a maximum extension of 2,200 m in north–northeast to south–southwest and 900 m in north–northwest to south–southeast directions. The lake basin has a steep sloping shoreline with slopes up to 25° and a 1,000 m by 500 m wide almost flat central part, which is down to 52 m deep. An arc-shaped ridge (*Barschbuckel*) of about 600 m length and 50–70 m width occurs in the southwestern part of the lake basin. We suggest this structure is part of a palagonized tuff ring. About 125 m north of the *Barschbuckel,* three humps each 4 m high on average with a diameter up to 60 m were identified. The origin of these structures is not yet understood and under investigation. Several deltas occur in the littoral zone of the lake basin and are linked to erosional processes along the crater wall. A major underwater slide occurred in the northwestern section of the lake body (loc. G in Fig. 5).

From horizontal gradients of elevation three former lake terraces can be distinguished and can be attributed to lake level regulations as water management measures in historical times.

At the time of our measurements in summer 2010, in the water body of *Laacher See,* three-layer stratification was established. Measured pH values are strongly dependent on the concentration of dissolved CO_2, which are highest close to the lake bottom. That means that amounts of the rising CO_2 gas bubbles get dissolved and CO_2 remains in the bottom water. The number of CO_2-degassing vents (wet mofettes) in the lake is considerably higher in the northern part of the *Laacher See* basin. Overall, the vent clusters form an almost circular-shaped (diameter of 1,500 m) pattern, tracing the crater rim of the northern eruption center of the *Laacher See Volcano*. The concentrically arranged clusters inside the crater rim are zones of preferential gas flow along conjugated sets of faults, which are caused by post-eruptive tectonic processes. At the eastern lake basin, the crater rim of the northern eruption center runs close to the shoreline, where CO_2-degassing vents occur on lakeside as well as landside (dry mofettes). Since wet mofettes do not occur at the northern lake, we suggest that the northern part of the northern crater rim extends onshore. The absence of degassing vents in the central northern lake is most likely related to the extent of a magma body below the lake, which is inhibiting gas rise. In the southern part of

the lake, CO_2-degassing vents occur in high spatial density only in a single area, close to the foot of the subaqueous fan of the creek *Beller Bach*. The cause of this isolated mofette cluster may be taken as proof for the conduit of the *Barschbuckel* palagonitic tuff ring.

References

Aeschbach-Hertig W, Kipfer R, Hofer M, Imboden DM, Wieler R, Signer P (1996) Quantification of gas fluxes from the subcontinental mantle: the example of Laacher See, a Maar Lake in Germany. Geochim Cosmochim Acta 60:31–41

Ahrens W (1932) Die Basaltvulkane des südöstlichen Laacher See Gebiets und ihre Lavaströme. Jahrb Preußische Geologische Landesanstalt 53:851–879

Anzidei M, Carapezza ML, Esposito A, Giordano G, Lelli M, Tarchini L (2008) The Albano Maar Lake high resolution bathymetry and dissolved CO_2 budget (Colli Albani volcano, Italy): constrains to hazard evaluation. J Volcanol Geotherm Res 171:258–268. doi:10.1016/j.jvolgeores.2007.11.024

Bahrig B (1985) Sedimentation und Diagenese im Laacher Seebecken. Bochumer geologische und geotechnische Arbeiten, 19, Bochum, 231 pp

Bernard A (2011) CO_2 degassing at Taal volcano. www.ulb.oc.be/sciences/cvl/taal/Taal.html. 10 August 2011

Canet C, Prol-Ledesma RM, Dando PR, Vázquez-Figueroa V, Shumilin E, Birosta E, Sánchez A, Robinson CJ, Camprubí A, Tauler E (2010) Discovery of massive seafloor gas seepage along the Wagner Fault, northern Gulf of California. Sediment Geol 228:292–303

Cardigos F, Colac A, Dando PR, Ávila SP, Sarradin P-M, Tempera F, Conceição P, Pascoal A, Serrão Santos R (2005) Shallow water hydrothermal vent field fluids and communities of the D. João de Castro Seamount (Azores). Chem Geol 224:153–168

Carlé W. (1975). Die Mineral- und Thermalwässer von Mitteleuropa. Geologie, Chemismus, Genese. Wissenschaftliche Verlagsgesellschaft mbH, Stuttgart, 643 pp

Duda A, Schmincke H-U (1978) Quaternary basanites, melilite nephelinites and tephrites from Laacher See area (Germany). J Mineral Geochem 132:1–33

Fornaciai A, Favalli M, Karátson D, Tarquini S, Boschi E (2012) Morphometry of scoria cones, and their relation to geodynamic setting: a DEM-based analysis. J Volcanol Geotherm Res. doi:10.1016/j.jvolgeores.2011.12.012

Frechen J (1971) Siebengebirge am Rhein—Laacher See Vulkangebiet—Maargebiet der Westeifel. Sammlung Geologischer Führer 56, Gebrüder Borntraeger, Berlin, 209 pp

Frechen J, Hopmann M, Knetsch G (1967) Die Vulkanische Eifel. Geologische Reihe, Stollfuß, Bonn, 140 pp

Freundt A, Schminke H-U (1984) Geologisch-vulkanologisches Gutachten zum Naturschutzgebiet Laacher See östlich des Laacher Sees, 1-111, unpublished report

Gal F, Brach M, Braibant G, Jouin F, Michel K (2011) CO_2 escapes in the Laacher See region, East Eifel, Germany: application of natural analogue onshore and offshore geochemical monitoring. Int J Greenh Gas Control 5:1099–1118

GARMIN (2012) GPSMAP 400/500 series: owner's manual, 78 pp

Giggenbach WF, Sano Y, Schmicke HU (1991) CO_2-rich gases from Lakes Nyos and Monoun, Cameroon; Laacher See, Germany; Dieng, Indonesia, and Mt. Gambier, Australia—variations on a common theme. J Volcanol Geotherm Res 45:311–323. doi:10.1016/0377-0273(91)90065-8

Goepel A (2008) Natürliche Gläser und Glasuren in den Vulkaniten der Westeifel. PhD thesis, Institute for Geosciences, Friedrich-Schiller University, Jena, 499 pp

Grewe K (1979) Der Fulbert Stollen am Laacher See. Eine Ingenieursleistung des hohen Mittelalters. Zeitschr Arch Mittelalt 7:107–142

Grosse P, van Wyk de Vries B, Euillades PA, Kervyn M, Petrinovic IA (2012) Systematic morphometric characterization of volcanic edifices using digital elevation models. Geomorphology 136:114–131

Guzzetti F, Mondini AC, Cardinali M, Fiorucci MS, Chang K-T (2012) Landslide inventory maps: new tools for an old problem. Earth Sci Rev 112:42–66

Harms E, Schmincke H-U (2000) Volatile composition of the phonolitic Laacher See magma (12,900 year BP): implications for syn-eruptive degassing of S, F, Cl, and H_2O. Contrib Miner Petrol 138:84–98

Hernández PA, Salazar JM, Shimoike Y, Mori T, Notsu K, Pérez NM (2001) Diffuse emission of CO_2 from Miyakejima volcano, Japan. Chem Geol 177:175–185

Hernández PA, Pérez N, Weber K, Fischer C, Bothe K, Laue M, Mebus R, Sumino H, Melián G, Padrón E (2010) Emisión difusa de CO_2 por el lago volcánico Laacher See, Alemania. Aportaciones recientes en volcanologia 2005–2008, ed., Centro de estudios Calatravos, ISBN: 978-84-614-1025-5

Lorenzen KF, Berckhemer H (1976) Das geomagnetische Feld im Gebiet des Laacher Sees. N. Jb. Geol. Paläont., Stuttgart, 197-208. In: Meyer W (1994) Geologie der Eifel. 3. Auflage, Schweizerbart`sche Verlagsbuchhandlung, Stuttgart, 618 pp

May F (2002) Quantifizierung des CO_2-Flusses zur Abbildung magmatischer Prozesse im Untergrund der Westeifel. Shakerverlag, Aachen, 170 pp

McGinnis DF, Schmidt M, DelSontro T, Themann S, Rovelli L, Reitz A, Linke P (2011) Discovery of a natural CO_2 seep in the German North Sea: implications for shallow dissolved gas and seep detection. J Geophys Res 116:C03013. doi:10.1029/2010JC006557

Meyer W (1994) Geologie der Eifel. 3. Auflage, Schweizerbart`sche Verlagsbuchhandlung, Stuttgart, 618 pp

Morgan LA, Shanks WC, Lovalvo DA, Johnson SY, Stephenson WJ, Pierce KL, Harlan SS, Finn CA, Lee G, Webring M, Schulze B, Dühn J, Sweeney R, Balistrieri L (2003) Exploration and discovery in Yellowstone Lake: results from high-resolution sonar imaging, seismic reflection profiling, and submersible studies. J Volcanol Geotherm Res 122:221–242. doi:10.1016/S0377-0273(02)00503-6

Padrón E, Hernández PA, Toulkeridis T, Pérez NM, Marrero R, Melián G, Virgili G, Notsu K (2008) Diffuse CO_2 emission rate from Pululahua and the lake-filled Cuicocha calderas, Ecuador. J Volcanol Geotherm Res 176:163–169. doi:10.1016/j.jvolgeores.2007.11.023

Pérez NM, Hernández PA, Padilla G, Nolasco D, Barrancos J, Melián G, Padrón E, Dionis S, Calvo D, Rodríguez F, Notsu K, Mori T, Kusakabe M, Arpa MC, Reniva P, Ibarra M (2011) Global CO_2 emission from volcanic lakes. Geology 39(3):235–238. doi:10.1130/G31586.1

Pfanz H (2008) Mofetten - Kalter Atem schlafender Vulkane. RVDL-Verlag, Köln, 85 pp, ISBN 978-3-86526-036-9

Pucher R (1992) Magnetfeldanomalien in der Eifel. Geol Rundsch 81(2):429–443

Ross KA, Smets B, De Batist M, Hilbe M, Schmid M, Anselmetti FS (2014) Lake-level rise in the late Pleistocene and active subaquatic volcanism since the Holocene in Lake Kivu; East African Rift. Geomorphology 221:274–285. doi:10.1016/j.geomorph.2014.05.010

Scharf BW (1987) Limnologische Beschreibung, Nutzung und Unterhaltung von Eifelmaaren. Ministerium für Umwelt und Gesundheit, Rheinland-Pfalz, 117 pp

Scharf BW, Menn U (1992) Hydrology and morphometry. In: Scharf BW, Björk S (eds) Limnology of Eifel maar lakes, Ergebnisse der Limnologie 38, Stuttgart, 348 pp

Scharf BW, Oehms M (1992) Physical and chemical characteristics. In: Scharf BW, Björk S (eds) Limnology of Eifel maar lakes, Ergebnisse der Limnologie 38, Stuttgart, 348 pp

Schmincke H-U (1977) Phreatomagmatische Phasen in quartären Vulkanen der Osteifel. Geol Jb A39:3–45

Schmincke H-U (1996) Vulkanismus im Laacher See Gebiet. Pluto Press, Ascheberg, 60 pp

Schmincke HU, Park C, Harms E (1999) Evolution and environmental impacts of the eruption of Laacher See Volcano (Germany) 12,900 a BP. Quatern Int 61:61–72

Stoiber-Lipp J, Wirth S, Tischer J, Gärtner S, Büchel G, Viereck L (2012) Kartierung von Trockenmofetten im Laacher See Becken. Ein-Blicke, Sonderband Deutsche Vulkanologische Gesellschaft e.V., 101-110, Mendig, ISBN: 978-3-86972-020-3

Takano B, Suzuki K, Sugimori K, Ohba T, Fazlullin SM, Bernard A, Sumarti S, Sukhyar R, Hirabayashi M (2004) Bathymetric and geochemical investigation of Kawah Ijen Crater Lake, East Java, Indonesia. J Volcanol Geotherm Res 135:299–329. doi:10.1016/j.jvolgeores.2004.03.008

Ulusoy I, Cubukcu E, Aydar E, Labazuy P, Gourgaud A, Vincent PM (2004) Volcanic and deformation history of the Bodrum resurgment caldera system (southwestern Turkey). J Volcanol Geotherm Res 136:71–96. doi:10.1016/j.jvolgeores.2004.03.016

van den Bogaard P, Schmincke H-U (1985) Laacher See tephra: a widespread isochronous late Quternary tephra layer in central and northern Europe. Geol Soc Am Bull 96:1554–1571

van den Bogaard P, Schmincke H-U (1990a) Die Entwicklungsgeschichte des Mittelrheinraumes und die Eruptionsgeschichte des Osteifel-Vulkanfeldes. In: Schirmer W (Hrsg) Rheingeschichte zwischen Mosel und Maas. *Deuqua-Führer*, 1, 166-190, Hannover

van den Bogaard P, Schmincke H-U (1990b) Geologische Karte der Osteifel, 1:25000. Pluto Press Witten, Kiel

Viereck L (1984). Geologische und petrologische Entwicklung des pleistozänen Vulkankomplexes Rieden, Ost-Eifel. Bochumer geologische und geotechnische Arbeiten, 17, Bochum, 337 pp

Wessels M, Bussmann I, Schloemer S, Schlüter M, Bödere V (2010) Distribution, morphology, and formation of pockmarks in Lake Constance, Germany. Limnol Oceanogr 55(6):2623–2633

Wilson WD (1960) Equation for the speed of sound in sea water. J Acoust Soc Am 32(10):1357